Diabetic dyslipidaemia is associated with alterations in eNOS, caveolin-1 and endothelial dysfunction in streptozotocin treated rats

Yousif A Shamsaldeen, Rosemary Ugur, Christopher D Benham and Lisa A Lione *

School of Life and Medical Sciences, University of Hertfordshire, College Lane, AL10 9AB, UK, email: l.lione@herts.ac.uk

*Corresponding Author

Lisa A Lione, School of Life and Medical Sciences, University Hertfordshire, College Lane, AL10 9AB, UK, Tel: +44 1707 286195; Fax: +44 1707 285046 email: l.lione@herts.ac.uk

Abstract (213 words)

Background: Diabetes is a complex progressive disease characterised by chronic hyperglycaemia and dyslipidaemia associated with endothelial dysfunction. Oxidised LDL (Ox-LDL) is elevated in diabetes and may contribute to endothelial dysfunction. The aim of this study was to relate the serum levels of Ox-LDL with endothelial dysfunction in streptozotocin (STZ)-diabetic rats and to further explore the changes in endothelial nitric oxide synthase (eNOS) and caveolin-1 (CAV-1) expression in primary aortic endothelial cells (ECs).

Methods: Diabetes was induced with a single intraperitoneal injection of STZ in male Wistar rats. During the hyperglycaemic diabetes state serum lipid markers, aortic relaxation and aortic ECs eNOS and CAV-1 protein expression was measured.

Results: Elevated serum Ox-LDL (STZ 1486 ± 78.1 pg/ml vs control 732.6 ± 160.6pg/ml, $p<0.05$) was associated with hyperglycaemia (STZ 29 ± 0.9 mmol/L vs control: 7.2 ± 0.2 mmol/L, $p<0.001$) and hypertriglyceridemia (STZ 9.0 ± 1.5 mmol/L vs control: 3.0 ± 0.3 mmol/L, $p<0.01$) in diabetic rats. A significant reduction was observed in STZ-diabetic aortic

endothelial cell eNOS and CAV-1 of 40% and 30% respectively, accompanied by a compromised STZ-diabetic carbachol-induced vasodilation (STZ 29.6 ± 9.3% vs control 77.2 ± 2.5%, p<0.001).

Conclusions: The elevated serum Ox-LDL in hyperglycaemic STZ-diabetic rats may contribute to diabetic endothelial dysfunction, possibly through downregulation of endothelial CAV-1 and eNOS.

Key words:

diabetes, oxidative LDL, endothelial nitric oxide synthase, caveolin-1, endothelial dysfunction

Abbreviations:

AGEs, advanced glycation end products;

STZ, streptozotocin;

Ox-LDL, oxidative low-density lipoprotein

HDL, high density lipoprotein

TGs, triglycerides

eNOS: endothelial nitric oxide synthase

CAV-1: caveolin-1

CC: carbachol

ECs: endothelial cells

NA: noradrenaline

1. Introduction (410 words)

The incidence of diabetes mellitus is increasing throughout the world and numbers are expected to reach 592 million by the year 2035, mainly because of the increase in obesity [1]. Despite the differences in aetiology, clinical presentation and disease prevalence, secondary complications, such as endothelial dysfunction, occur in both type 1 and 2 diabetes. Diabetes complications are largely resistant to treatments posing a huge economic burden to the health system and society. Endothelial dysfunction renders diabetics vulnerable to limb infections and end-organ damage such as nephropathy, neuropathy as well as retinopathy [2]. As yet, there are no biomarker predictors to indicate endothelial dysfunction in diabetes.

In recent decades, strategies for managing vascular complications associated with diabetes have moved away from a "glucocentric" approach to address additional risk factors that contribute to the development and progression of atherosclerosis. The presence of an atherogenic lipid profile is common in diabetic patients and is characterised by elevated plasma triglyceride (TGs) levels, low levels of high-density lipoprotein (HDL)-cholesterol and a preponderance of small dense LDL particles. Oxidised LDL (Ox-LDL) is a key component in the genesis of the atherosclerotic lesion and is cytotoxic to various cell types including endothelial cells (ECs) and therefore is suggested to contribute to endothelial dysfunction [3]

Caveolae form highly organised microdomains in the ECs plasma membrane through providing docking sites for numerous signalling molecules, such as endothelial nitric oxide synthase (eNOS) [4]. Caveolin-1 (CAV-1) is a principal protein and marker found in the endothelial caveolae [5] and is co-localised with eNOS in cultured bovine aortic ECs [6]. Furthermore, both CAV-1 and eNOS are significantly downregulated in diabetic kidneys [7] linked to decreased renal eNOS-derived nitric oxide and diabetic cavernosal tissues decreased NO mediated relaxation leading to erectile dysfunction [8]. Disruption of endothelial caveolae

leading to eNOS uncoupling and diminished flow-mediated dilation in coronary arterioles of diabetic patients has also been observed [9].

We have previously shown that abnormal vascular responsiveness in STZ-diabetic rats are attributed in part to the overproduction of reactive oxygen species [10]. Here we aim to investigate the alteration in non-HDL, HDL, Ox-LDL, cholesterol and TGs serum concentrations, and whether it is associated with changes in the expression of eNOS and CAV-1 proteins in endothelial cell together with aortic vascular dysfunction using the STZ-diabetic rat model.

2. Materials and Methods (1552 words)

2.1 Materials and Reagents

Streptozotocin (STZ, S-0130) was purchased from Sigma-Aldrich (UK). Ox-LDL sandwich ELISA (SEA527Ra) were from Cloud clone corp. LDL, HDL, cholesterol and TGs Randox (Rx) Monza kits (CH 202, CH 203) were from Randox (www.randox.com). All culture reagents were from Fischer Scientific. The rabbit primary antibody for eNOS (PA3-031A) and CAV-1 (PA5-17447) were obtained from Thermo Fisher Scientific. The fluorescence goat secondary anti rabbit antibody (FI-1000) was obtained from Vector laboratories. All other chemicals were of analytical grade and were obtained from local companies.

2.2 Induction of diabetes

This study was approved by the Institutional Animal Welfare and Ethics review committee and conducted in accordance with guidelines established by the Animals Scientific

Procedures Act, 1986 and European directive 2010/63/EU carried out under project licence PPL70/7732. Male Wistar rats (325-425g, Charles River, UK) were given a single injection of 65mg/kg Streptozotocin (STZ, Dose volume 10ml/kg); dissolved in 20 mM citrate buffer (pH 4.5) intraperitoneally. Control rats received injections of citrate buffer alone. Animals were housed in pairs with water and food (5LF2 10% protein LabDiet, switched to 5LF5 22% protein Labdiet on day of STZ injection) freely available throughout the study. For 48 hours following STZ or control injection, 2% sucrose solution was also provided to avoid the initial hypoglycaemia that is seen following STZ. Diabetes was confirmed on day 7 and terminal day (in the 2nd week post-injection) by testing a drop of tail vein blood, obtained by a needle prick of conscious rats, measured using an Accu-check blood glucose monitor. Rats showing an elevated blood glucose of >16mmol/L on day 7 were considered diabetic. Rats were euthanized by schedule 1 procedure (CO_2 asphyxiation) and thoracic aorta blood was sampled and left to coagulate in Eppendorf tubes before being centrifuged at 13000rpm for 5 minutes. The supernatant (the serum) was then transferred to another Eppendorf tube and stored at -80°C for up to 12 months. Aortas were freshly isolated for vasoactive responses or endothelial cell isolation and primary culture.

2.3 Oxidative LDL (Ox-LDL) determination in serum

All samples were analysed through sandwich ELISA according to the manufacturer's instructions (Cloud clone corp, SEA527Ra). The OxLDL ELISA assay has high sensitivity and specificity for detection of Oxidized Low-Density Lipoprotein (OxLDL) with a detection range of 31.25-2000pg/mL. The immunogen used in the ELISA is native protein of Cu^{2+} oxidized LDL.

2.4 Non HDL, HDL, TGs, cholesterol determination in serum

Serum samples were analysed for HDL, cholesterol and TGs using Randox (Rx) Monza kits according to the manufacturer's instructions (www.randox.com, CH 202, CH 203). Prior to assaying each marker, calibrations were carried out and all samples were allowed to thaw on ice, centrifuged at 4000 rpm for 5 min and kept on ice until assay. Briefly, for total serum cholesterol, 500ul of Chol R1 reagent was mixed with 50ul of serum sample, left at $37^{o}C$ for 10 min. For serum HDL, 500ul of HDL R1a precipitant reagent was inverted with 200ul serum sample and left to stand at room temp for 10min. The sample was then centrifuged at 4000rpm for 10min and 50ul supernatant added to 500ul of Chol R1 reagent, left at $37^{o}C$ for 10min. For serum TGs, 500ul of R1b reagent was mixed with 5ul serum sample, left at $37^{o}C$ for 10 min. All prepared samples were then transferred into semi micro-cuvettes and absorbance levels read at 510nm (HDL, Chol) and 546nm (TGs). The Friedewald equation cannot be used when TGs values are ≥ 400 mg/dl because it tends to underestimate absolute LDL concentrations [11]. Given the elevated TGs (approximately 9 mmol/ 797 mg/dl) in our STZ rats non high-density lipoprotein (non-HDL) cholesterol concentrations (which includes very-low-density lipoprotein VLDL, intermediate-density lipoprotein IDL and low-density lipoprotein LDL), were calculated by subtracting the HDL cholesterol from total cholesterol values.

2.5 Aortic vascular function

Aortic endothelial function was evaluated in STZ-diabetic rats and control rats (in the 2nd week post-injection). Briefly, freshly isolated aorta was cut into approximately 2-3mm wide rings which were threaded by superior and inferior loops where the inferior thread loop was attached to a fixed hook and kept suspended in a Bennett isolated tissue organ bath filled with Krebs solution pH 7.4 at $37°C\pm1°C$ and gassed with 95% O_2/ 5% CO_2. The superior loop was attached through long terminal thread to FT-100 force transducer under 1g tension

force. FT-100 force transducer transmitted tissue response to iWORKS amplifier that generated electrical signals to be recorded through Labscribe software from iWORKS (version 1.817). Thereafter, aortic rings were left to equilibrate for 60-90 minutes with approximately 15 minutes washing intervals. Aortic rings were then pre-contracted with noradrenaline (Sigma Aldrich, A7257) (NA; 300nM) before being treated with carbachol (CC) (Sigma Aldrich, C4328) to generate a cumulative concentration response curve (30nM-300μM).

2.6 Expression of eNOS and CAV-1 in Primary endothelial cells

Cell studies were conducted to determine the expression level of eNOS and CAV-1 in primary rat aortic ECs (in the 2nd week post-injection) through laser scanning confocal microscopy (LSCM) based immunocytochemistry. Primary aortic ECs were isolated aseptically. Briefly, rat aorta was freshly isolated and plunged into sterile Hank's balanced salt solution (HBSS) (Fisher-Scientific, 10227632). The aorta was cleaned from the connective tissue (de-adventitia) using autoclaved forceps and scissors and cut into small rings (2-3mm long). Afterward, the aortic rings were transferred into a sterile tube containing warm serum free medium 199 (Fisher-Scientific, 10696733) (10ml) containing collagenase (1 mg/ml) (Sigma Aldrich, C1639) and agitated for 90 minutes at 37°C. Afterward, 1 ml of new born calf serum (Fisher-Scientific, 10014173) was added to the collagenase activity. A wide mouth pipette was used to forcibly flush the aortic rings to dislodge any possible loosely hanging ECs. The aortic rings were then discarded and the media 199 that contains new born calf serum, collagenase and ECs was then centrifuged for 5-minutes at 10000rpm at 25°C. The supernatant was discarded and the small pellet containing ECs was then re-suspended in collagenase free media 199 (3ml). The re-suspended pellet was then plated on rat tail collagen (Type I) (Fisher-Scientific, C7661) coated t-25 flask and the flask was left in the

incubator (5% CO2, 37°C) for 25-30 minutes. The media was then aspirated, and the recently

adhered cells were washed twice with HBSS to remove any possible impurities, debris or

aortic smooth muscle cells (ASMCs). The flask was then added with complete DMEM (low

glucose 1 g/L) (3ml) (Fisher-Scientific, 10135082) containing horse serum (15%) and

newborn calf serum (4%), endothelial cell growth factor 75micg/ml (Fisher-Scientific,

E0760), and heparin powder (0.005% w/v) (Fisher-Scientific, H3149) in addition to

streptomycin-penicillin 1x (Fisher-Scientific, 10101043). The ECs were grown to

approximately 80% confluence within 7 days. Afterward, the confluent primary ECs were

trypsinised (Fisher-Scientific, 10217723) and seeded on autoclaved poly-L-lysine (Sigma

Aldrich, P4932) coated glass coverslips (0.16-0.19mm thick). ECs were grown on the

coverslips for two days till reaching approximately 70% confluency. The ECs were labelled

with acetylated low-density lipoprotein (dil-Ac-LDL) as recommended by the manufacturer

(Alfa Aesar, BT-902). The acetylated-LDL is taken-up selectively by the ECs that hydrolyse

the acetyl bond to release the fluorescence LDL which is trapped intracellularly, endowing

red fluorescence to the ECs.

The coverslips were then incubated with paraformaldehyde (4% in HBSS pH 7.4) in

the dark at room temperature for 1 hour to fix the ECs. Afterward, the ECs were permealised

through Triton-X100 (0.5% in HBSS) incubation for 10 minutes in the dark at room

temperature. The coverslips were washed 3 times with HBSS. The ECs were incubated with

rabbit primary antibody (1:100) for eNOS (Thermo Fisher Scientific, PA3-031A) or CAV-1

(Thermo Fisher Scientific, PA5-17447) in blocking solution composed of phosphate buffer

saline pH 7.4, bovine serum albumin (BSA) (Sigma Aldrich, A9418) (1%) and foetal calf

serum (FCS) (Thermo Fisher Scientific, 10500-064) (2%) for overnight in 4°C. Thereafter,

the ECs were washed with HBSS before being incubated with the fluorescence goat

secondary anti rabbit antibody (Vector laboratories, FI-1000) (1:1000) for 2 hours at room

temperature. The coverslips were then washed with HBSS and mounted on microscope glass slides with a drop of mounting media containing DAPI (Vector laboratories, H-1500) which stains the nucleus in blue. The ECs were visualised with Nikon C1 CLSM and EZ-C1 silver version 3.9 software. The images are then uploaded to ImageJ 1.46r software for quantitative analysis. The expression of eNOS and CAV-1 was quantified through measuring the fluorescence intensity per cell (n= 3-4 cells/coverslip), and then normalised to the intensity of the control cells for each antibody.

2.7 Statistical analysis

All data are expressed as mean ± standard error of the mean (SEM). 'n' refers to independent values, not replicates. Data subjected to statistical analysis have n of at least 4/group. Data was analysed by either an unpaired t test or repeated measures or two-way ANOVA followed by Bonferroni's post-hoc test, using GraphPad prism version 5.00. Differences were considered to be statistically significant when $p=<0.05$. p values lower than 0.05 are expressed as $P<0.01$ or 0.001. Carbachol (CC, 30nM- 300µM) induced relaxation of aortic rings is normalized to % relaxation of noradrenaline EC_{80} (300nM) contraction in STZ-diabetic rats' aortic rings and control rats' aortic rings. Primary aortic ECs were plated onto poly-l-lysine coated glass coverslips and visualised under LSCM. The confocal microscopy representative images were quantitatively analysed through ImageJ software (version 1.46r) and statistically analysed through Graph Pad prism (version 5.00).

3. Results (524 words)

3.1 Effect of STZ on serum glucose, non-HDL, Ox-LDL, TGs, HDL and cholesterol

Administration of STZ resulted in hyperglycaemia in all rats by day 7 and was sustained throughout the study. Blood glucose was significantly elevated in STZ-diabetic rats (> four-fold) as early as day 7 compared with age-matched control rats (STZ-diabetic: 29 ± 0.9

mmol/L; control: 7.2 ± 0.2 mmol/L $p<0.001$, Figure 1). Animal health was closely monitored daily, and it was noted that although the STZ- diabetic animals failed to increase body weight they did manage to maintain their starting weights (data not shown). All STZ diabetic animals showed typical symptoms of the disease such as polydipsia, polyuria, glycosuria as well as hyperglycaemia (data not shown).

Compared with the control group, the levels of Ox-LDL and TGs were significantly increased in serum from STZ-diabetic rats (Figures 2b, c). Serum non-HDL cholesterol in STZ-diabetic rats just failed to reach significance compared with control rats ($p=0.1$, Figure 2a) whilst TGs increased three-fold (Figure 2c). A small but significant increase in total serum cholesterol was noted (Figure 2e), although serum HDL cholesterol remained unchanged in STZ-diabetic rats compared with controls (Figure 2d).

3.2 Effect of STZ on carbachol induced aortic vascular relaxation

The increase in Ox-LDL and TGs was accompanied by a significant STZ-diabetic aortic dysfunction as shown in Figure 3. Aortic rings pre-contracted with 300nM noradrenaline from STZ-diabetic rats showed a significant increase in vasoconstriction (0.37 ± 0.02g, *$P<0.05$) compared with control rat aorta (0.30 ± 0.02g,) and a significant decrease in vascular relaxant response to carbachol ($EC_{50}= 0.8 \pm 0.4\mu M$ & $E_{max}= 29.6 \pm 9.3\%$, *** $P<0.001$) compared with control rat aorta ($EC_{50}= 0.6\mu M \pm 0.2\mu M$ & $E_{max} = 77.2 \pm 2.5\%$). In separate experiments control rat aortic rings pre-incubated with L-NAME (100μM) for 30 minutes (Emax = $11.3 \pm 1.6\%$), and when endothelium was denuded (Emax = $12.5 \pm 4.7\%$), both showed a significant decrease (*** $P<0.001$) in vascular relaxation in response to carbachol when compared with control rat aorta (Emax = $77.2 \pm 2.5\%$, data not shown). These data provide a causal link between altered nitric oxide synthase and altered aortic vasorelaxation.

3.3 Effect of STZ on aortic endothelial cell eNOS staining

To investigate whether the reduced aortic vasorelaxation response in STZ-diabetic rats might be due to dysfunction in nitric oxide (NO) generation by endothelial cells (ECs) we investigated primary cultures of ECs from control and STZ-diabetic rat aorta. The LSCM images of EC cells stained with eNOS antibody showed distinct distribution of eNOS around the nucleus and at the edges of the plasma membrane (indicated by yellow arrows in Figure 4a). Control ECs showed significantly higher eNOS expression compared to STZ-diabetic ECs (control N=5 average expression $100.0 \pm 4.3\%$ vs STZ-diabetic N=6, $62.1 \pm 5.8\%$) (Figure 4c).

3.4 Effect of STZ on aortic endothelial cell CAV-1 staining

Caveolae are 50- to 100-nm diameter lipid raft invaginations in the endothelial cells membrane. Caveolae form approximately 95% of the ECs surface invaginations and function as a signalling platform that facilitates interactions of signalling molecules [12]. Among the signalling molecules docked in the caveolae is eNOS [6]. CAV-1 is a major protein component of the endothelial caveolae. Previous studies have shown that eNOS and CAV-1 are co-localised in rat kidneys and cultured bovine aortic endothelial cells [6, 7]. Accordingly, we hypothesised that the levels of eNOS and CAV-1 proteins are altered in STZ-diabetic rat aortic ECs. Immunocytochemistry studies were conducted which showed significant CAV-1 downregulation and disruption in STZ-diabetic aortic ECs (Figure 5a, b). Total CAV-1 expression showed a significant reduction in STZ-diabetic rat aortic ECs compared with control rat aortic ECs (Control, N=5 average expression $100.0 \pm 3.0\%$ vs STZ N=4, $73.8 \pm 4.3\%$) (Figure 5c).

Discussion (1132 words)

In this study, STZ-diabetic rats developed symptoms of diabetes such as hyperglycaemia by day 7 which was sustained over 24 days (Figure 1), consistent with others

[13]. Furthermore, we have previously shown endothelial dysfunction is evident as early as 8 days following STZ injection and hence lipid markers and endothelial dysfunction were measured during the 2nd week post STZ injection in this study [14].

Herein, we demonstrated a state of hyperlipidaemia (elevation of serum TGs, cholesterol, Ox-LDL) in this type 1 model of diabetes. Compared with the control group, the levels of Ox-LDL and TGs were significantly increased in serum from STZ-diabetic rats (Figure 2). However, serum non-HDL cholesterol (which include LDL, VLDL, ILDL) levels in STZ rats, although elevated, did not show a significant difference when compared with control levels (p=1.0). TGs increased three-fold in serum in line with the four-fold increase in blood glucose (Figure 2). A small but significant increase in total cholesterol was noted, although HDL levels remained unchanged, in STZ-diabetic rats compared with controls (Figure 2). This hyperlipidaemia is consistent with previous findings in non-insulin treated type 1 diabetic patients [15] and type 1 diabetes models (with no insulin replacement therapy) [16, 17]. The elevated serum TGs and Ox-LDL in STZ-diabetic rats may be attributed to increased production and decreased clearance of triglyceride-rich lipoproteins. In adipose tissues, insulin suppresses lipolysis by inhibiting the activity of hormone sensitive lipase, which catalyses the mobilisation of free fatty acids from stored TGs [18]. The STZ-mediated destruction of the pancreatic β-cells results in an insulinopaenic state in STZ-diabetic rats and hence the lack of insulin will result in an increased lipolysis of triglyceride-rich lipoproteins (LDL, TGs) and furthermore given carbohydrates can no longer be utilised efficiently as an energy source this leads to a greater reliance on energy from fat and protein to meet the energy demands of the animal [19].

Similar to previous findings in type 2 diabetic patients, we observed a relationship between serum Ox-LDL concentrations and serum TGs concentrations in our STZ-diabetic rats [18]. In patients with type-2 diabetes, hyperglycaemia enhances the oxidative stress, further

modifying LDL into Ox-LDL, which is likely occurring in our type 1 hyperglycaemic STZ diabetic rats. This association is seen even in healthy volunteers where transiently increased plasma glucose levels correlates with higher oxidation of LDL [20]. Moreover, an inverse relationship has been observed between LDL sizes and circulating Ox-LDL in type 2 diabetic patients [21]. In fact, the formation of small, dense LDL particles is mostly observed in hypertriglyceridaemic states [22]. Therefore, both the increase in triglycerides and oxidation of LDL in our STZ type 1 diabetic rats indicates that there may be a predominance of small dense LDL (increased number of LDL particles). Small dense LDL particles are likely to be taken up more easily across the endothelium into the arterial wall, compared to larger LDL particles. Studies often express levels of Ox-LDL in different formats and units of measurement (e.g. in mg/dl) [23] as in our study, or Ox-LDL to total LDL [18]. Further different assays use antibodies detecting different epitopes on Ox-LDL, so caution needs to be applied when interpreting results and comparing across studies [24].

Our dyslipidaemic STZ-diabetic rats showed endothelial dysfunction through impaired cholinergic-induced endothelium-dependent aortic vasodilation (Figure 3) consistent with [25]. Increased circulating Ox-LDL in our STZ-diabetic rats may directly damage arteries, possibly via the Ox LDL receptor, LOX-1, which is up-regulated in the vascular endothelium of diabetic animals, leading to foam cell formation and plaque development, as a causal relationship between Ox-LDL and atherosclerosis is well established [26]. Moreover, an increased Ox-LDL/apoB ratio has been associated with macrovascular disease and peripheral neuropathy in Japanese patients with type 2 diabetes [18]. Ox-LDL molecules are recognised by the CD36 endothelial scavenger receptor that facilitates the uptake and the endocytosis of Ox-LDL [27]. Ox-LDL molecules are cholesterol acceptors that compete with caveolae to deplete the caveolae from cholesterol and hence causes caveolae disruption displacing eNOS [28]. Such caveolae disruption would inhibit eNOS attachment to CAV-1 and subsequent eNOS activation

[28] therefore yielding endothelial dysfunction, as observed seen in our STZ diabetic rats (Figure 3) and depicted in Figure 6. Furthermore, the elevated serum Ox-LDL in our STZ-diabetic rats may directly inhibit eNOS attachment to CAV-1 and hence reduce the eNOS coupling with CAV-1 that culminates in compromised eNOS activity and subsequent NO release and vasodilation [29].

In support of this hypothesis, our immunocytochemistry studies showed significant downregulation of eNOS and CAV-1 in cultured primary STZ-diabetic aortic ECs (Figures 4 & 5). Additionally, eNOS showed corresponding distribution to CAV-1 in control aortic ECs, perinuclear and at the edges of the plasma membrane (Figures 4 & 5) revealing the overlapping distribution of these two essential elements, consistent with Wang et al. [6] findings of eNOS and CAV-1 co-localisation in bovine aortic ECs. Interestingly this downregulation is not consistent with Elçioğlu et al., [30] who report an increased expression of CAV-1 in STZ-diabetic aorta, although their Western blots of whole aorta is likely to indicate accumulation of CAV-1 protein in the predominant vascular smooth muscle cells rather than endothelial cell caveolae. These authors note STZ impairs aortic vascular relaxation, but they do not investigate CAV-1 expression in aortic ECs. This is the first report of STZ-diabetes induced eNOS and CAV-1 downregulation in primary rat aortic ECs.

Disruption of endothelial caveolae and reduced CAV-1 has been found in coronary arteries of diabetic patients, and in human coronary endothelial cells under high glucose, linked to ONOO (-) formation and eNOS uncoupling and diminished flow-mediated dilation [9]. There is limited information on functional interactions of CAV-1 and eNOS in the microdomain. The decrease in CAV-1 and eNOS aortic EC expression in diabetes may lead to a decrease in eNOS activity and NO release, resulting in impaired endothelium dependent aortic vasodilation. This finding might be attributed to inhibited phosphatidylinositol 3-kinase/Akt (PI3K-Akt) pathway since PI3K inhibitor, wortmannin was shown to inhibit the

eNOS and CAV-1 translocation to the plasma membrane in bovine aortic ECs [6] (Figure 6). Interestingly, the 3-hydroxy-3-methyl-glutaryl-CoA reductase inhibitors, simvastatin and lovastatin protect eNOS activity from Ox-LDL-induced downregulation [31]. HDL binds mainly on scavenger receptor class B isoform I (SR-BI) where it delivers the circulating cholesterol to the caveolae maintaining the caveolae integrity and enhancing eNOS activity which may support a benefit for increasing the HDL/Cholesterol ratio [32]. The mechanism of CAV-1 and eNOS downregulation and reduced eNOS activity in diabetic aortic ECs needs further investigation.

Conclusion

In summary, STZ-diabetic rats showed significant endothelial dysfunction demonstrated by impaired carbachol-induced vasodilation. Such endothelial dysfunction was accompanied by eNOS and CAV-1 downregulation in STZ-diabetic aortic primary ECs. STZ-diabetic rats showed a significant increase in serum Ox-LDL level which may contribute to the oxidative and carbonyl stress associated with diabetic eNOS and CAV-1 endothelial dysfunction.

Acknowledgements

Author Contributions

YS, CB and LL conceived and designed the experiments; YS and RU performed the experiments; YS, RU and LL analysed the data; YS, CB and LL wrote and proofread the paper. All authors read and approved the final manuscript.

Conflict of Interest

The authors declare that there is no conflict of interest associated with this publication.

References:

1. Diabetes UK. *Diabetes: Facts and Stats.* Diabetes UK. 2014; 3:1-21.

2. American Diabetes Association. Diagnosis and Classification of Diabetes Mellitus. *Diabetes Care*. 2012;35(1):S64-S71.

3. Hessler JR, Robertson AL, Chisolm GM. LDL-induced cytotoxicity and its inhibition by HDL in human vascular smooth muscle and endothelial cells in culture. Atherosclerosis. 1979;32(3):213-29.

4. Garland CJ, Hiley CR, Dora KA. EDHF: spreading the influence of the endothelium. *Br J Pharmacol*. 2011; 164: 839-852.

5. Frank PG, Woodman SE, Park DS, Lisanti MP. Caveolin, caveolae, and endothelial cell function. *Arterioscler Thromb Vasc Biol*. 2003; 23(7):1161-8.

6. Wang H, Wang AX, Liu Z, Chai W, Barrett EJ. The Trafficking/Interaction of eNOS and Caveolin-1 Induced by Insulin Modulates Endothelial Nitric Oxide Production. *Molecular Endocrinology*. 2009; 23(10):1613–23.

7. Komers R, Schutzer WE, Reed JF, Lindsley JN, Oyama TT, Buck DC, et al. Altered Endothelial Nitric Oxide Synthase Targeting and Conformation and Caveolin-1 Expression in the Diabetic Kidney. *Diabetes.* 2006;55(6):1651-9.

8. Park, C.S., Ryu, S.D., Hwang, S.Y., Elevation of intracavernous pressure and NO cGMP activity by a new herbal formula in penile tissues of aged and diabetic rats. *J. Ethnopharmacol*. 2004; 94, 85–92.

9. Cassuto J1, Dou H, Czikora I, Szabo A, Patel VS, Kamath V, Belin de Chantemele E, Feher A, Romero MJ, Bagi Z. 2014. Peroxynitrite disrupts endothelial caveolae leading to eNOS uncoupling and diminished flow-mediated dilation in coronary arterioles of diabetic patients. *Diabetes*. 2014; 63(4):1381-93.

10. ur Rehman A, Dugic E, Benham C, Lione L, Mackenzie LS. Selective inhibition of NADPH oxidase reverses the over contraction of diabetic rat aorta. *Redox Biology*. 2014; 2:61-4.

11. Nauck M, Warnick GR, Rifai N. 2002. Methods for measurement of LDL-cholesterol: a critical assessment of direct measurement by homogeneous assays versus calculation. *Clin Chem*. 2002; 48(2):236-54.

12. Yao X, Garland CJ. Recent Developments in Vascular Endothelial Cell Transient Receptor Potential Channels. *Circulation Research*. 2005; 97(9):853-63.

13. Wei M, Ong L, Smith MT, Ross FB, Schmid K, Hoey AJ, et al. The Streptozotocin-Diabetic Rat as a Model of the Chronic Complications of Human Diabetes. *Heart Lung & Circulation*. 2003;12(1):44-50.

14. Shamsaldeen Y, Lione LA and Benham C. Decrease in TRPV4 Expression in Vascular Endothelium From STZ Treated Rats is Reversed by Insulin Treatment, *pA2 online* 2015; 13 (3) 011P.

15. Pérez A, Wägner AM, Carreras G, Giménez G, Sánchez-Quesada JL, Rigla M, et al. Prevalence and Phenotypic Distribution of Dyslipidemia in Type 1 Diabetes Mellitus. *JAMA*. 2000; 160(18):2756-62.

16. Harano Y1, Kojima H, Kosugi K, Suzuki M, Harada M, Nakano T, Hidaka H, Kashiwagi A, Torii R, Taniguchi Y, Hyperlipidemia and atherosclerosis in experimental insulinopenic diabetic monkeys. *Diabetes Res Clin Pract*. 1992;16(3):163-73.

17. Amalan V, Vijayakumar N, Indumathi D, Ramakrishnan A. Antidiabetic and antihyperlipidemic activity of p-coumaric acid in diabetic rats, role of pancreatic GLUT 2: In vivo approach. *Biomed Pharmacother*. 2016; 84:230-236.

18. Tsuzura S, Ikeda Y, Suehiro T, Ota K, Osaki F, Arii K, et al. Correlation of plasma oxidized low-density lipoprotein levels to vascular complications and human serum paraoxonase in patients with type 2 diabetes. *Metabolism.* 2004; 53(3):297–302.

19. Shamsaldeen YA, Mackenzie LS, Lione LA, Benham CD. 2016. Methylglyoxal, A Metabolite Increased in Diabetes is Associated with Insulin Resistance, Vascular Dysfunction and Neuropathies*. Current Drug Metabolism.* 2016;17(4):359-67.

20. Chen N, Azhar S, Abbasi F, Carantoni M, Reaven G. The relationship between plasma glucose and insulin responses to oral glucose, LDL oxidation, and soluble intercellular adhesion molecule-1 in healthy volunteers. *Atherosclerosis*. 2000; 152(1):203-8.

21. Scheffer PG, Bos G, Volwater HGFM, Dekker JM, Heine RJ, Teerlink T. Associations of LDL size with in vitro oxidizability and plasma levels of in vivo oxidized LDL in Type 2 diabetic patients. *Diabetic Medicine.* 2003; 20(7):563-7.

22. Deckelbaum RJ, Granot E, Oschry Y, Rose L, Eisenberg S. Plasma triglyceride determines structure-composition in low and high density lipoproteins. *Arteriosclerosis, Thrombosis, and Vascular Biology*. 1984; 4(3):225-31.

23. Holvoet P1, Vanhaecke J, Janssens S, Van de Werf F, Collen D. Oxidized LDL and malondialdehyde-modified LDL in patients with acute coronary syndromes and stable coronary artery disease. *Circulation*. 1998;98(15):1487-94.

24. Levitan I, Volkov S, Subbaiah PV. Oxidized LDL: diversity, patterns of recognition, and pathophysiology. *Antioxidants & redox signaling*. 2010; 13(1):39-75.

25. Fukao M, Hattori Y, Kanno M, Sakuma I, Kitabatake A. Alterations in endothelium-dependent hyperpolarization and relaxation in mesenteric arteries from streptozotocin-induced diabetic rats. *British Journal of Pharmacology*. 1997; 121(7):1383-91.

26. Shah S, Casas J-P, Drenos F, Whittaker J, Deanfield J, Swerdlow DI, Causal relevance of blood lipid fractions in the development of carotid atherosclerosis: Mendelian randomization analysis. *Circ Cardiovasc Genet*. 2013; 6(1):63-72.

27. Zeng Y, Tao N, Chung KN, Heuser JE, Lublin DM. Endocytosis of Oxidized Low Density Lipoprotein through Scavenger Receptor CD36 Utilizes a Lipid Raft Pathway That Does Not Require Caveolin-1. *The Journal of Biological Chemistry*. 2003; 278(46):45931–6.

28. Blair A, Shaul PW, Yuhanna IS, Conrad PA, Smart EJ. Oxidized Low Density Lipoprotein Displaces Endothelial Nitric-oxide Synthase (eNOS) from Plasmalemmal Caveolae and Impairs eNOS Activation. *The Journal of Biological Chemistry.* 1999; 274:32512-9.

29. Shaul PW, Smart EJ, Robinsoni LJ, German Z, Yuhanna IS, Ying Y, et al. Acylation Targets Endothelial Nitric-oxide Synthase to Plasmalemmal Caveola. The *Journal of Biological Chemistry.* 1996; 271(11):6518-22.

30. Elçioğlu KH, Kabasakal L, Cetinel S, Conturk G, Sezen SF, Ayanoğlu-Dülger G. Changes in caveolin-1 expression and vasoreactivity in the aorta and corpus

cavernosum of fructose and streptozotocin-induced diabetic rats. *Eur J Pharmacol.* 2010; 642(1-3):113-20.

31. Laufs U, Fata VL, Plutzky J, Liao JK. Upregulation of Endothelial Nitric Oxide Synthase by HMG CoA Reductase Inhibitors. *Circulation*. 1998; 97:1129-35.

32. Yuhanna IS, Zhu Y, Cox BE, Hahner LD, Lawrence SO, Lu P, et al. High-density lipoprotein binding to scavenger receptor-BI activates endothelial nitric oxide synthase. *Nature Medicine*. 2001; 7:853-7.
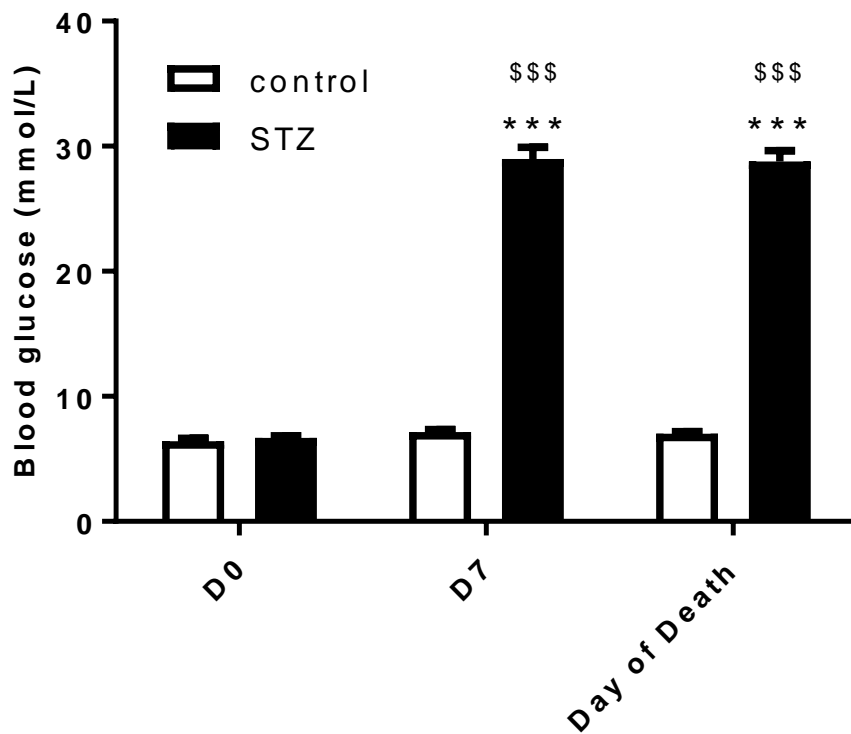

Figure 1. Effect of STZ diabetes on blood glucose (mmol/L) at day 0, day 7 and day of death (2nd week post injection). Significantly different from control group is denoted by ***= $p<0.001$, $$$=$p<0.001$ versus day 0 using unpaired Student t-test. Data are presented as mean $\pm$ S.E.M (control n=16, STZ n=24).
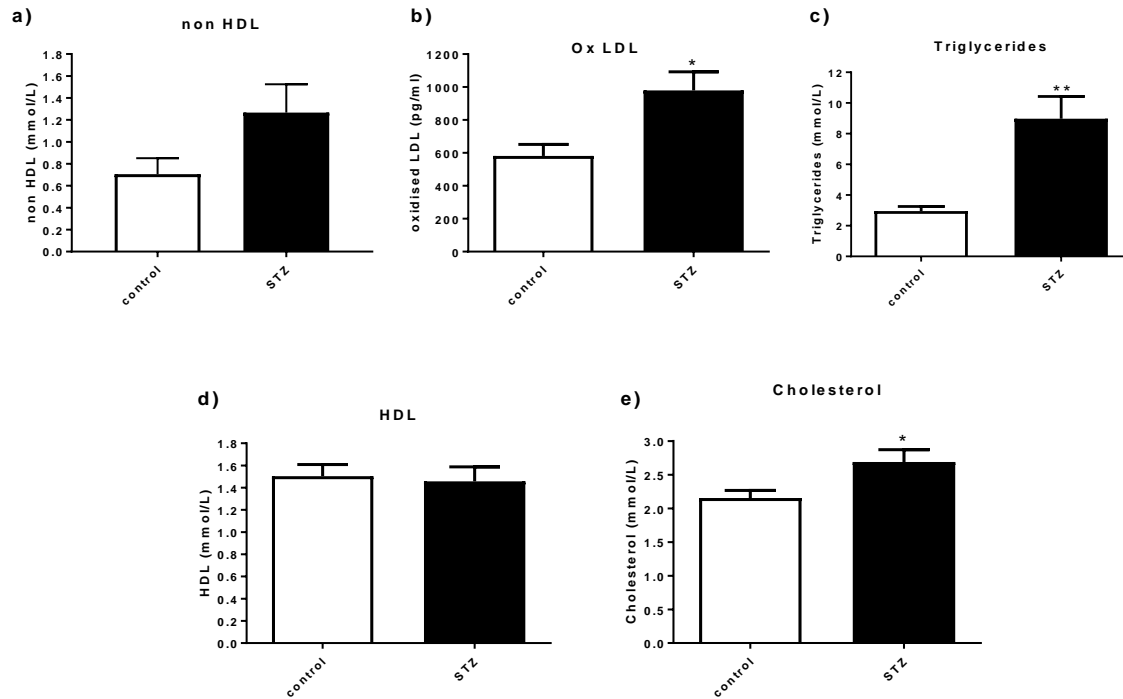
Figure 2. Effect of STZ diabetes on: a) serum non-HDL (mmol/L) b) serum Ox-LDL (pg/ml) c) serum TGs (mmol/L) d) serum HDL (mmol/L) and e) serum total cholesterol (mmol/L) at 2nd week post injection. Data are presented as mean ± S.E.M (n=4 for Ox-LDL; n=24 for all other serum markers). Significance is denoted by *= $p<0.05$, **=$p<0.01$ different from control group, using unpaired 2-tailed t test. Serum non-HDL (panel a) STZ versus control was close to significance at p=0.1.
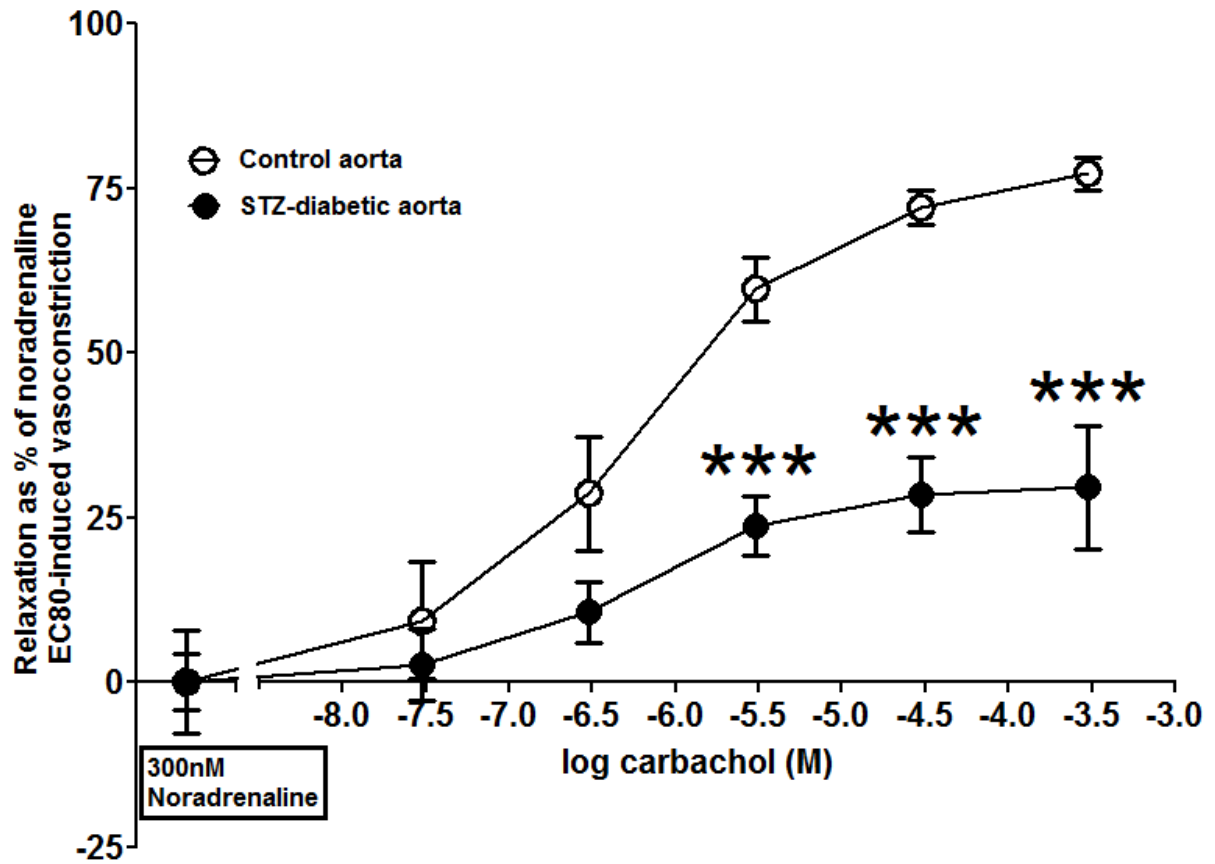
Figure 3. Concentration response curves to carbachol mediated relaxation, normalized (%) to Noradrenaline (NA) EC_{80} (300nM) contraction in aorta rings from STZ-diabetic rats vs control rats at 2nd week post injection. Data were analysed through Bonferroni's two-way repeated measures ANOVA. Data presented as mean ± SEM (N=5-6). Significance is represented as *** $P<0.001$ versus control. FBC: final bath concentration.
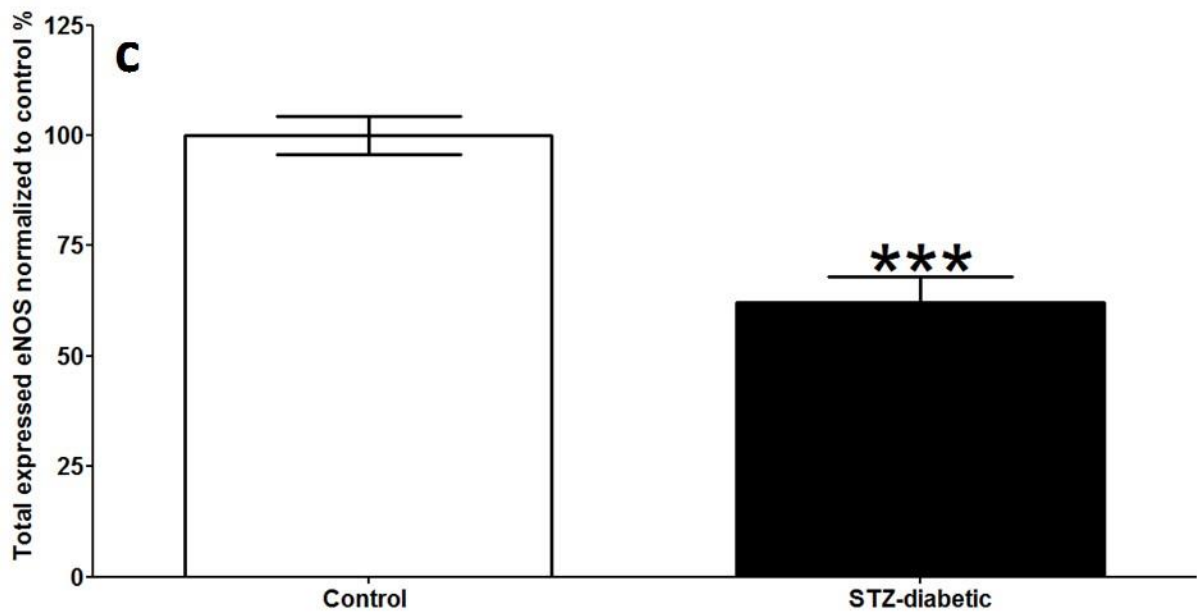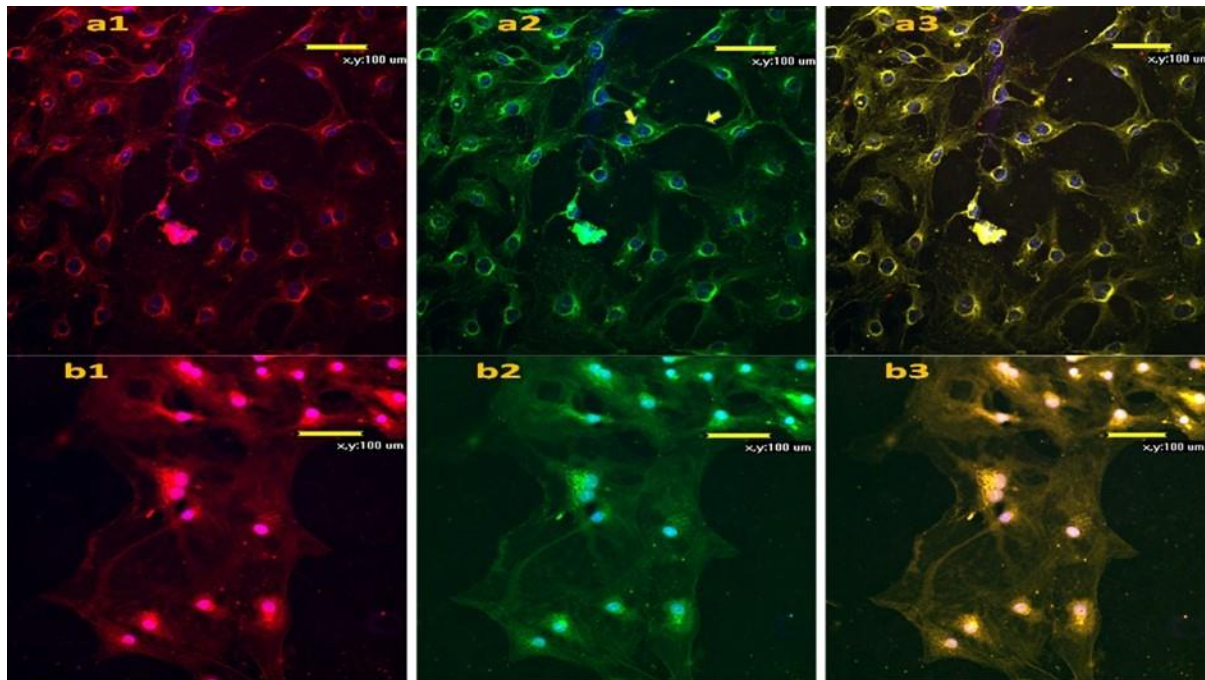
Figure 4. eNOS expression in primary endothelial cells from control and diabetic rat aorta under laser scanning confocal microscope. Panels a and b are control and STZ diabetic aortic endothelial cells respectively. Endothelial cells were probed with DAPI to label the nucleus in blue and marked with acetylate oxidised LDL (Ac-Ox-LDL) giving the cells the red colour (a1 & b1). Anti eNOS primary antibody probed with secondary fluorescence antibody

showed distinct distribution around the nucleus and at the edge of plasma membrane in control naïve aortic endothelial cells as pointed by the arrows (a2). STZ-diabetic endothelial cells showed disrupted eNOS distribution with less fluorescence light emission (b2). Images were combined to merge endothelial marker (red), nucleus marker (blue) and eNOS fluorescence antibody (green) (a3 & b3). c) Quantitative analysis of eNOS immunoreactivity. Data is mean +/- SEM (N= 5-6) of total eNOS expression (% of control) in rat aortic endothelial cells. STZ diabetic ECs showed a significant reduction in eNOS expression compared with control aortic ECs. Significance is represented as *** $P<0.001$ versus control when analysed through two tailed unpaired student t-test.
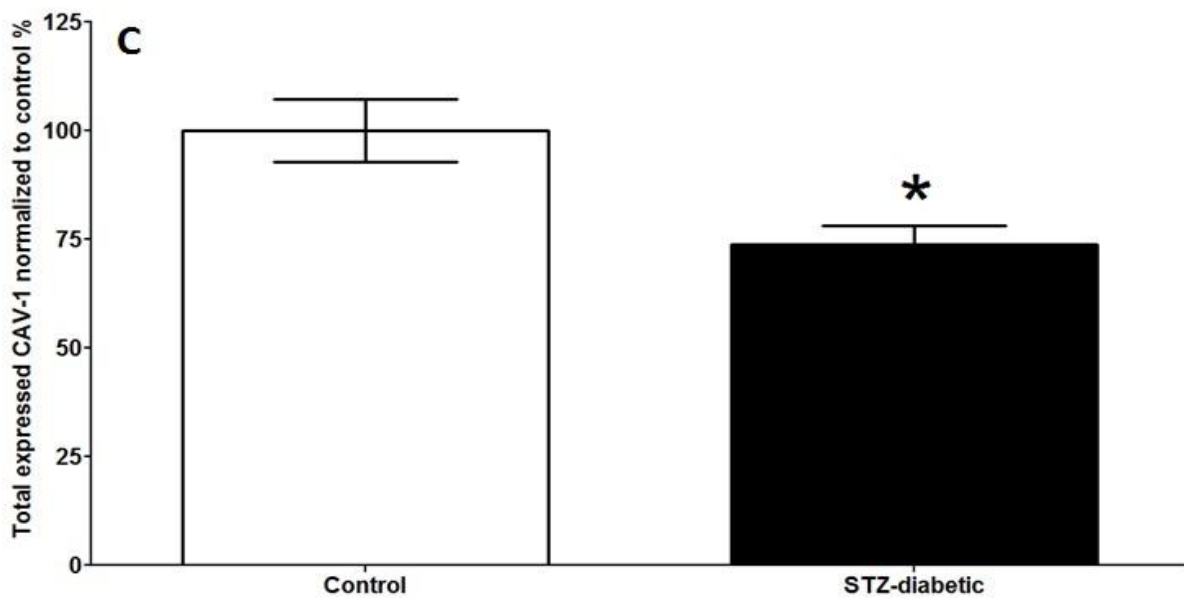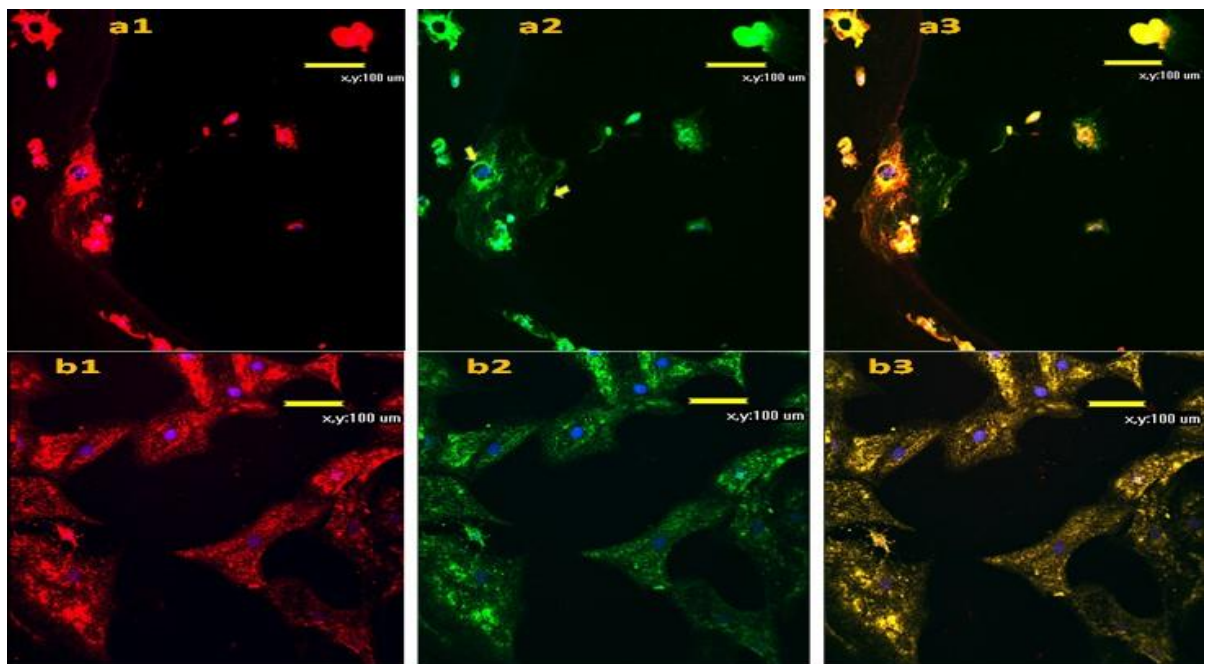
Figure 5. Caveolin-1 (CAV-1) expression in primary endothelial cells under laser scanning confocal microscope. Panels a and b are control and STZ diabetic aortic endothelial cells respectively. Endothelial cells were probed with DAPI to label the nucleus in blue and marked with acetylate oxidised LDL (Ac-Ox-LDL) giving the cells the red colour (a1 & b1). Anti caveolin-1 primary antibody probed with secondary fluorescence antibody showed distinct CAV-1 distribution around the nucleus and at the edge of plasma membrane in control aortic

ECs as labelled with yellow arrows (a2). STZ-diabetic ECs showed disrupted CAV-1 distribution with less fluorescence light emission (b2). Images were combined to merge endothelial marker (red), nucleus marker (blue) and CAV-1 fluorescence antibody (green) (a3 & b3). c) Data is mean +/- SEM (N=4-5) of total CAV-1 expression (% of control) in rat aortic endothelial cells. STZ diabetic ECs showed a significant reduction in CAV-1 expression compared with control aortic ECs. Significance is represented as * P<0.05 versus control when analysed through two tailed unpaired student t-test.
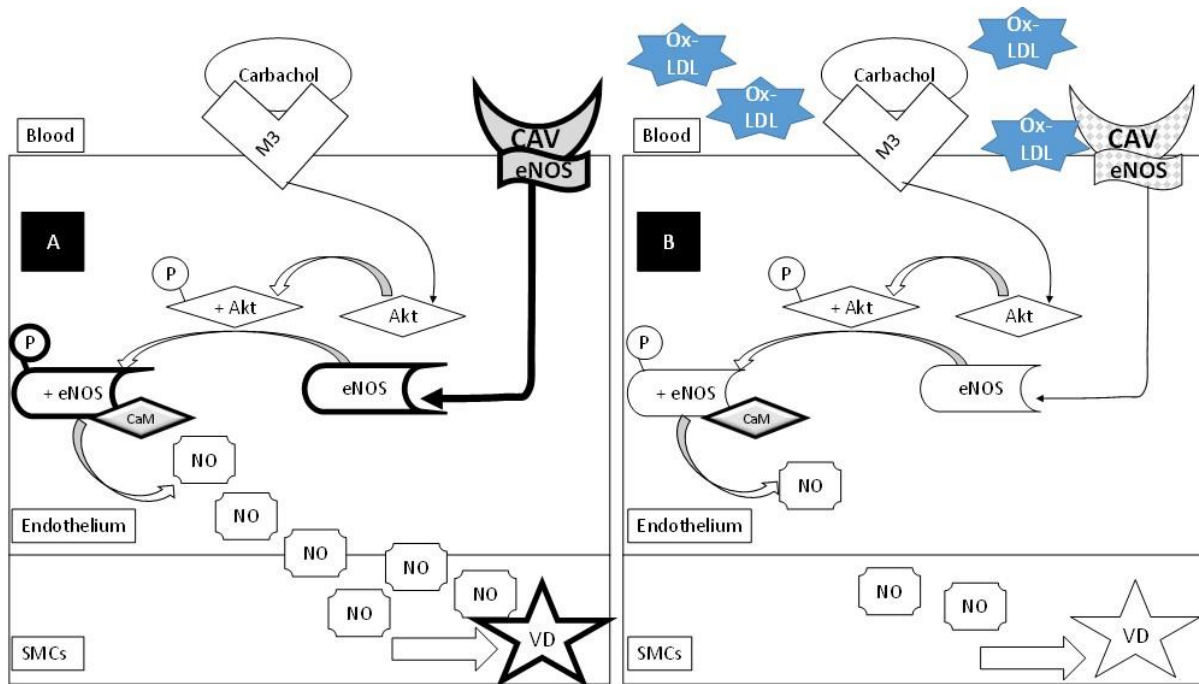
Figure 6. Schematic depiction of Ox-LDL effects and potential mechanisms underlying diabetic vascular dysfunction. Panel A depicts cholinergic induced aortic endothelium dependent vasodilation. Panel B depicts dysfunctional cholinergic induced aortic endothelial dependent vasodilation following STZ. NO: nitric oxide; CAV: caveolin-1; eNOS: endothelial nitric oxide synthase; Ox-LDL: oxidised low-density lipoprotein; VD: vasodilation; CaM: calmodulin; SMCs; smooth muscle cells.